Sickle Cell Anemia: Reference Values of Cerebral Blood Flow Determined by Continuous Arterial Spin Labeling MRI

M. ARKUSZEWSKI[1,2], J. KREJZA[3,4], R. CHEN[3], E.R. MELHEM[3]

[1] Department of Radiology, Division of Neuroradiology, University of Pennsylvania; Philadelphia, PA, USA
[2] Department of Neurology, Medical University of Silesia; Katowice, Poland
[3] Department of Diagnostic Radiology and Nuclear Medicine, University of Maryland School of Medicine; Baltimore, MD, USA
[4] Al-Imam Muhammad Ibn Saud Islamic University; Riyadh, Saudi Arabia

Key words: sickle cell anemia, brain, perfusion, magnetic resonance, tolerance limits

SUMMARY – *Sickle cell anemia (SCA) is a chronic illness associated with progressive deterioration in patients' quality of life. The major complications of SCA are cerebrovascular accidents (CVA) such as asymptomatic cerebral infarct or overt stroke. The risk of CVA may be related to chronic disturbances in cerebral blood flow (CBF), but the thresholds of "normal" steady-state CBF are not well established. The reference tolerance limits of CBF can be useful to estimate the risk of CVA in asymptomatic children with SCA, who are negative for hyperemia or evidence of arterial narrowing. Continuous arterial spin labeling (CASL) MR perfusion allows for non-invasive quantification of global and regional CBF. To establish such reference tolerance limits we performed CASL MR examinations on a 3-Tesla MR scanner in a carefully selected cohort of 42 children with SCA (mean age, 8.1±3.3 years; range limits, 2.3–14.4 years; 24 females), who were not on chronic transfusion therapy, had no history of overt stroke or transient ischemic attack, were free of signs and symptoms of focal vascular territory ischemic brain injury, did not have intracranial arterial narrowing on MR angiography and were at low risk for stroke as determined by transcranial Doppler ultrasonography.*

Introduction

Sickle cell anemia (SCA) affects millions of people in Africa, the Mediterranean region, the Middle East, India, the Caribbean and the Americas. SCA is a chronic illness associated with progressive deterioration in patients' quality of life [1,2]. The major complications of SCA are cerebrovascular accidents (CVA) such as overt stroke and silent cerebral infarcts (SCI) [3,4]. The high risk of CVA is a consequence of reduced oxygen delivery to the brain as a result of stenosis of major arteries supplying the brain or thromboembolic events.

It has been postulated that in steady-state SCA the brain is normally oxygenated due to a compensatory increase in cerebral blood flow (CBF) [5]. However, some recent studies did not detect increased CBF in some patients at high risk for stroke [6]. An inverse relationship between intracranial blood flow velocity [7] or cerebral perfusion (Arkuszewski M. and Krejza J - unpublished data) with the occurrence of SCI has been observed. The high risk of CVA can be related therefore to both high and low values of CBF, hence reference tolerance limits of CBF can be useful to estimate the risk. These tolerance limits can inform an investigator what CBF values may occur in relatively "healthy" children with SCA, who are without hyperemia or evidence of arterial narrowing.

Continuous arterial spin labeling (CASL) MR perfusion can provide a new means for risk assessment in asymptomatic children with SCA. It allows for non-invasive quantification of global and regional CBF by using magnetically labeled water molecules in arterial blood, without the need for exogenous agents [8,9]. CASL MR perfusion has shown promise as a sensitive indicator of CBF abnormalities in children
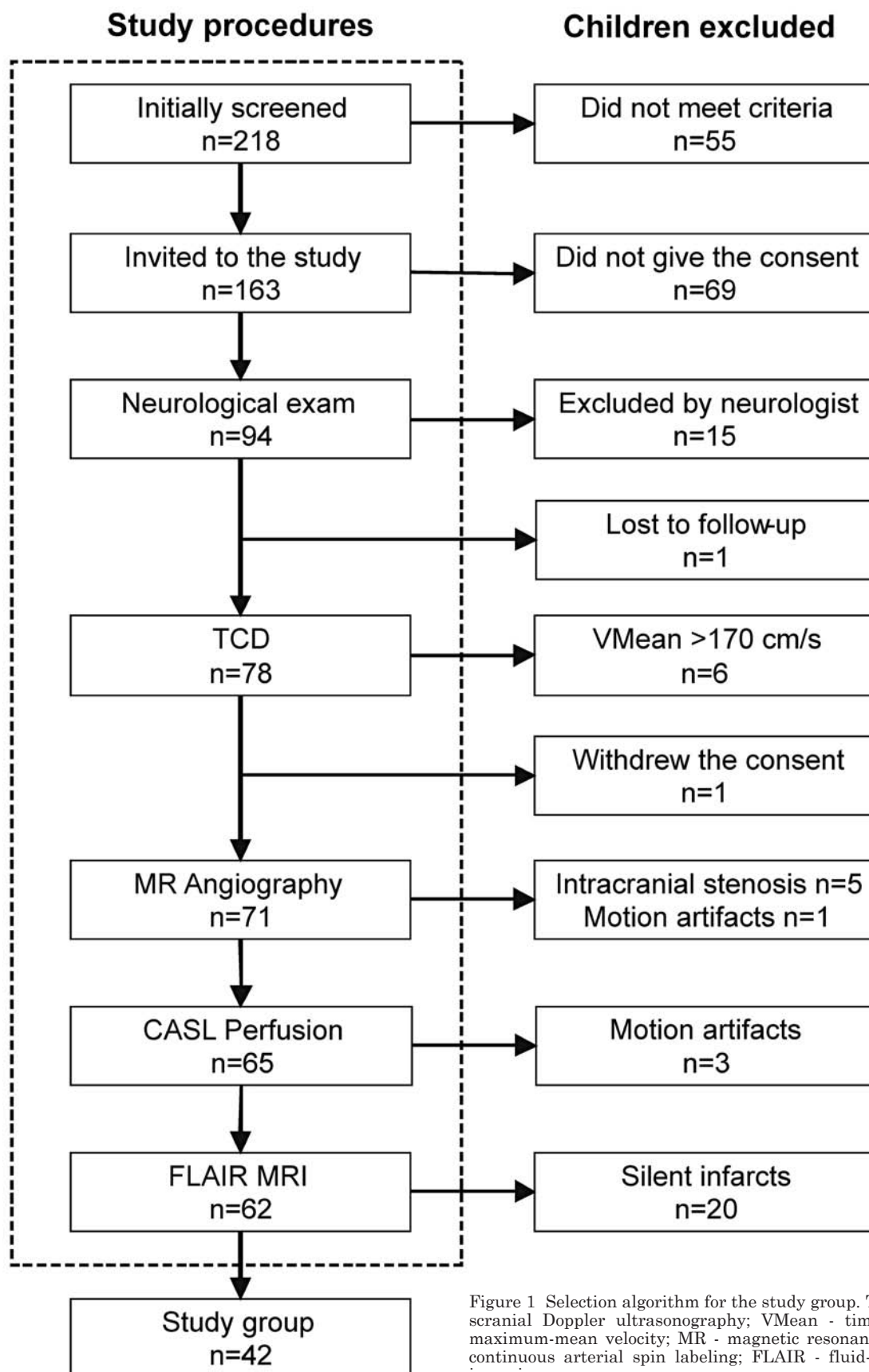
Study procedures   Children excluded

Figure 1 Selection algorithm for the study group. TCD - transcranial Doppler ultrasonography; VMean - time-averaged maximum-mean velocity; MR - magnetic resonance; CASL - continuous arterial spin labeling; FLAIR - fluid-attenuated inversion recovery.

in whom TCD and MR imaging findings are normal [10-12]. Thus, this study provides reference tolerance limits for CBF based on CASL MR data from children with SCA, who were not on chronic transfusion therapy, had no history of overt stroke or TIA, were free of signs or symptoms of focal vascular territory ischemic brain injury, did not have intracranial arterial narrowing on MR angiography (MRA) and who were at low risk for stroke as determined by transcranial Doppler ultrasonography (TCD).

Subjects and Methods

Study Group

Our cohort was recruited from within the Sickle Cell Ongoing Radiology Evaluation (SCORE) study funded by the National Institutes of Health. Our Institution's review board approved the protocol of this prospective study that was also compliant with the Health Insurance Portability and Accountability Act. Written informed consent was given by the subjects' parents with an assent provided by subjects seven years and older.

Children were recruited using the following inclusion criteria: 1) homozygous for the sickle cell gene (SS), confirmed by DNA–based mutational analysis; 2) two to 14 years of age; 3) absence of localizing abnormalities on neurologic examination indicating prior vascular territory ischemic injury; 4) no history of clinically overt stroke or TIA; and 5) conventional TCD examination performed at the screening. Exclusion criteria were the following: 1) history of major head injury requiring a visit to an emergency department; 2) history of seizure disorder requiring anticonvulsant therapy; 3) chronic transfusion therapy; 4) occurrence of acute chest syndrome or other significant acute illness in the period between blood laboratory and imaging studies; 5) history of prenatal or perinatal hypoxic-ischemic brain injury; 6) evidence of human immunodeficiency virus infection; 7) pregnancy; and 8) mean flow velocity >170 cm/s in any of major intracranial arteries on a screening routine TCD examination at entry to the study.

Clinical Assessment

After a standard comprehensive neurological examination by a pediatric neurologist, all qualifying children underwent TCD and imaging studies. Hemoglobin concentration (Hgb) and hematocrit level (Hct) were obtained during well visits closest in time to imaging studies. If hematology data were unavailable within 30 days of the study, we used an average of Hgb and Hct values from the three closest well visits because children were at steady-state. Twenty-three (55%) children had hematologic studies performed within 30 days of imaging examination. The median time from Hct and Hgb measurements to imaging studies was 24 days (range limits, 0-170 days).

TCD

TCD studies were performed independently of MRI by one of three sonographers, each with >5 years of experience, by using a single-channel portable unit (Pioneer TC 8080; Nicolet Vascular, Madison, WI, USA) equipped with a hand-held transducer operated in a range-gated pulse-waved mode at 2 MHz. The studies were performed while the children were awake; no sedation was used. TCD studies were performed using a standard approach through a temporal acoustic window. Blood flow Doppler signal intensity in the terminal portion of the internal carotid, middle and anterior cerebral arteries was detected using an adjustable operating depth at 2 mm increments and the sample volume size of 8-10 mm in the axial and 5 mm in the lateral direction [13]. Time-averaged maximum mean velocities were obtained by automatic tracing of the outline of Doppler waveforms.

Neuroimaging Studies

Prior to neuroimaging studies, all children younger than six years of age were sedated with oral chloral hydrate (75 to 100 mg/kg). Sedation was necessary because children under the age of six years have difficulty holding still for the length of the MR examination. Throughout the imaging period, children's heart rate (HR), capillary blood oxygen saturation (SPO_2) and systolic (SBP) and diastolic (DBP) blood pressure measurements were obtained using MRI compatible devices. Mean arterial pressure (MAP) was calculated according to formula MAP = 1/3 SBP + 2/3 DBP.

MRA

To exclude children with intracranial arterial stenosis, we performed a time-of-flight (TOF) 3D gradient-echo sequence (TR/TE =
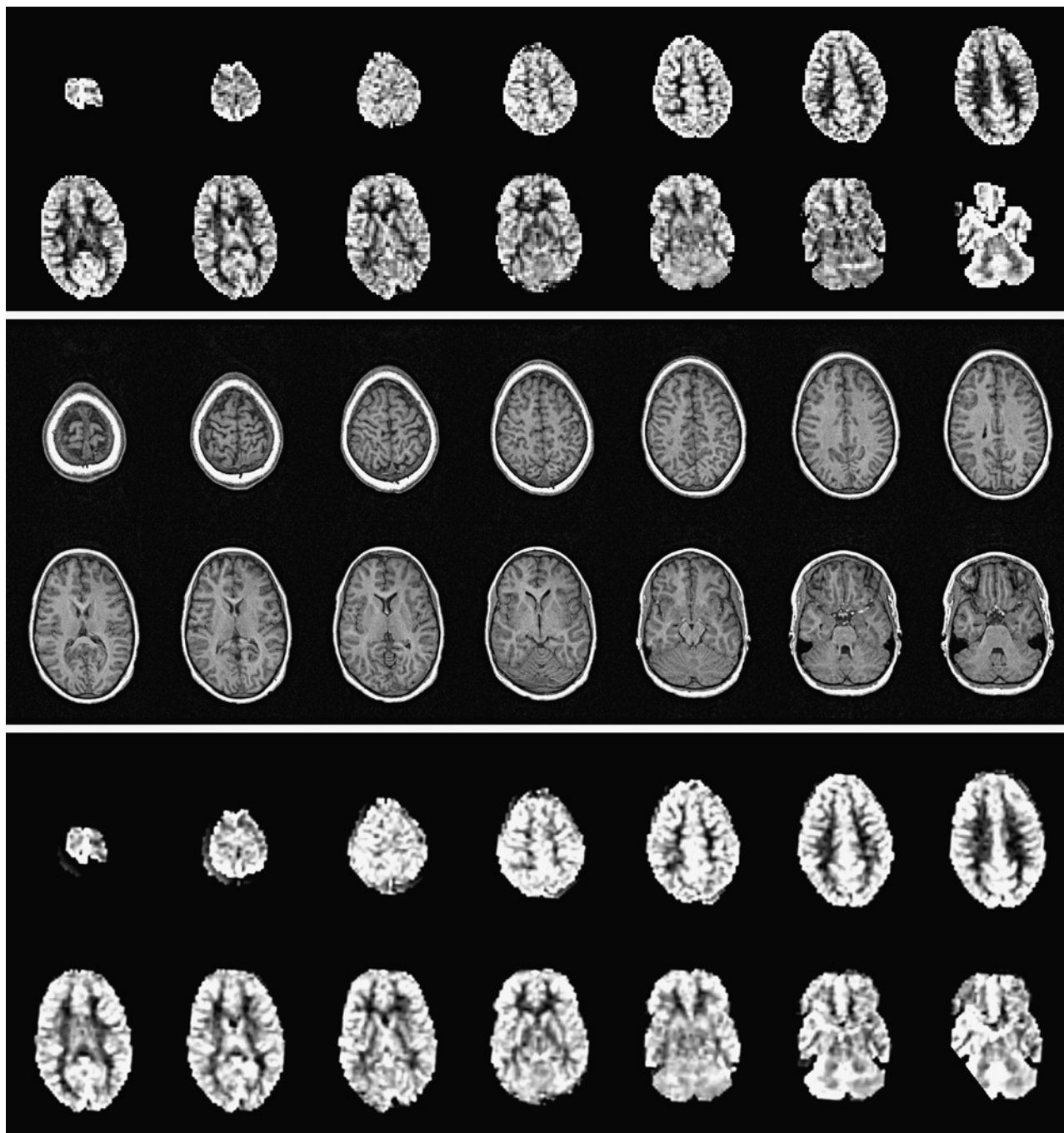
Figure 2 MR study of 9.7-year-old boy with sickle cell anemia. Top sequence: raw continuous arterial spin labeling (CASL) images registered at 1.2 s post-labeling delay. Middle sequence: anatomic T1 images. Bottom sequence: co-registration of the CASL and T1 sequences and quantification of cerebral blood flow (CBF) during off-line post processing. Averaged total-brain CBF is 97 ml/100g/min and inter-hemispheric difference is 3 ml/100g/min.

28/3.28 ms, flip angle = 25°; matrix = 512 × 448) on a 3T scanner (3-Tesla Magnetom Trio; Siemens, Erlangen, Germany) covering the intracranial arteries in the axial plane. Raw data from TOF MRA were transferred to an on-line workstation for the generation of segmented 2D arterial reprojections by using a commercially available maximum intensity projection ray trace and multiplanar reconstruction algorithms. The segmented 2D reprojections and

raw data of the intracranial part of the internal carotid arteries and branches of the circle of Willis were displayed on a 1024×1024 pixel-display workstation and evaluated independently by two pediatric neuroradiologists (both with more than 15 years of experience in angiography) unaware of the sonographic findings. Each evaluated all studies, and discrepancies were resolved by consensus.

Anatomical MR Imaging of the Brain

To detect silent infarctions, the whole brain MR imaging (MRI) (3-Tesla Magnetom Trio; Siemens, Erlangen, Germany) with a fast fluid attenuated inversion recovery (fast FLAIR) sequence was performed because of its superior demonstration of supratentorial T2-hyperintense lesions compared to other T2-weighted MR sequences. Two experienced neuroradiologists, each with more than 20 years of experience, blinded to patient data and results of other studies, independently identified silent infarcts defined as an area of abnormal hyperintensity on FLAIR images which was ≥3mm in diameter and was visible in at least two perpendicular planes. Discrepancies were resolved by consensus.

CASL Perfusion

Brain MR perfusion imaging was performed on the same MR machine using the CASL method originally described by Alsop *et al.* [8,9] Slice orientation was parallel to the anterior commissure - posterior commissure (AC-PC) plane. Perfusion sensitization was obtained using a single send-receive head coil. A 2.4 s long RF pulse (amplitude = 3.5∓T; gradient strength = 2.5 mT/m) was applied simultaneously with gradient at the level of the cervicomedullary junction to achieve flow-driven, adiabatic electromagnetic labeling of arterial spins in both carotid and vertebral arteries. To control for magnetization transfer (MT) effects, a reference image was acquired with sinusoidal modulation of the RF envelope with a frequency of 250 Hz, thereby achieving the simultaneous inversion of two parallel planes leading to a net zero degree on the labeled arterial water spins. This method allows for control of MT artifacts throughout the entire brain, thus enabling the performance of whole brain perfusion imaging. In order to reduce the sensitivity of the method to arterial transit time, the acquisition was delayed by 1.2 s after the labeling pre-pulse. A flow-compensated single-shot spin-echo echo planar (TR: 5000 ms, TE: 36 ms) readout was used to obtain fifteen 8 mm thick axial slices separated by a 1 mm gap with an in-plane resolution of 3.75×3.75 mm^2. The slices were acquired in an ascending order to reduce the remaining intravascular labeled spins by its natural crushing effect. Fifty pairs of labeled and control volumes were acquired consecutively to enhance signal-to-noise ratio for a total acquisition time of 10 min. MR perfusion images were sent to an off-line workstation for further post-processing. In order to produce high quality whole brain perfusion images on children, the following post-processing procedure was implemented using IDL (Research System Inc, Boulder, CO, USA). First, pair-wise subtraction of 50 labeled and control images was performed. The mean and standard deviation (SD) of the absolute difference between control and labeled images were calculated, and pairs showing an averaged subtracted signal larger than 2 SD were discarded from the final averaging, under the assumption that this large signal in the subtracted image was mainly due to motion artifacts. In a further step, each individual pair of subtracted images was screened visually to further remove dubious pairs of labeled-control images. The major advantage of this method is its robustness in discarding any signal that might not be due primarily to perfusion. The absolute CBF values (given in ml/100g/min) were calculated for each voxel and were further averaged for the whole brain and separately for each hemisphere. Because of possible motion artifacts, examinations with a proportion of negative pixels >.05 were excluded.

Statistical Analyses

We used the statistical software SYSTAT 12 (SPSS Science, Chicago, IL, USA), GraphPad free software (GraphPad, La Jolla, CA, USA; http://www.graphpad.com), and R statistical computing software (http://www.r-project.org/) to analyze data. Perfusion parameters were treated for outliers by using Grubbs t statistics at an α level <.05. We used Lilliefors' test provided by SYSTAT to check for the normality of the perfusion data. The distribution of the values fit normal distribution, thus perfusion values between hemispheres were first compared using a paired two-sided t test. A Pearson correlation coefficient (r) was used to quantify between-sides relationships of CBF, and
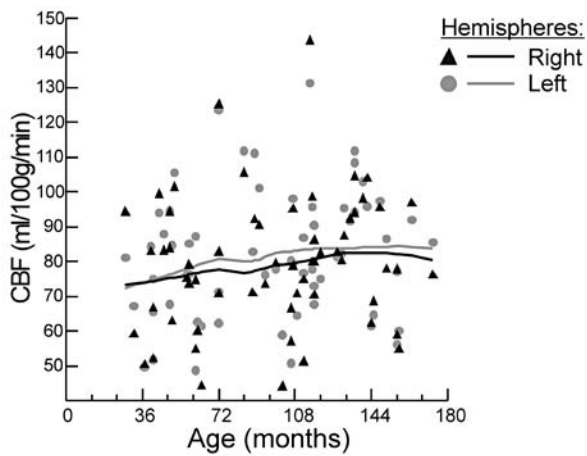
Figure 3 Graph shows an association of the averaged hemispheric cerebral blood flow values, as determined with continuous arterial spin labeling magnetic resonance imaging, with age in 42 children with sickle cell anemia, who had transcranial Doppler ultrasonography blood flow velocities in the intracranial arteries <170 cm/s. The distance-weighted least-squares smoothing method was used to calculate averaging curves.

the relationship of the CBF with parameters of systemic circulation. Sex differences in age, hematology values and perfusion parameters were analyzed using a two-sample *t* test with unequal variances and using the Mann-Whitney *U* test for non-normally distributed data. A similar approach was used in analyzing differences between CBF values between sedated and non-sedated children.

We used estimates of tolerance intervals, which have a probability of 0.90 of containing 95% of the population, to determine the reference values of the CBF parameters [14]. Because CBF values followed Gaussian distribution, we calculated the Gaussian tolerance interval. If L1 and L2 are the lower and upper limits of the interval, then L1=$\bar{x}$–ks, L2=$\bar{x}$+ks, where values of *k* were taken from an article by Weissberg and Beatty [15], $\bar{x}$=mean, *s*=SD.

Univariable and multivariable linear regression analysis was used to determine associations of perfusion values with age after adjustment for Hgb, Hct and systemic circulation parameters. Using a distance-weighted least-squares smoothing method, we computed curves for the mean CBF and age relation. A probability of <.05 was considered significant.

Results

The number of children excluded and the reasons for exclusion are shown in Figure 1. Seventy-one children underwent MR studies. Subsequently, based on MR results, 29 patients were excluded from further calculations of reference intervals because of presence of intracranial arterial narrowings (n=5), white matter

lesions (n=20), and motions artifacts (n=4). The final group consisted of 42 children (mean age, 8.1~3.3 years; range limits, 2.3-14.4 years; 24 females, 18 males). There was no difference between males and females in the age or mean values of hematologic or systemic hemodynamic variables, except sex difference in the HR (Table 1). Also, there were no differences in hematologic or systemic hemodynamic variables between sedated and not-sedated children.

Cerebral CASL MR Perfusion

The mean values and Gaussian tolerance limits of CBF parameters for total brain volume and for each hemisphere are given in Table 2 and an example of acquired CASL MR images is shown in Figure 2. There was no significant inter-hemispheric difference in the mean CBF (Table 2). CBF values from both hemispheres were significantly correlated (r=0.89, p<.001). No significant sex differences were found in total whole brain and hemispheric CBF values. We did not find any association between total brain and hemispheric CBF values with age also after controlling for Hct or Hgb, HR, SBP, DBP, MAP and SPO_2 or sedation factor. Despite no significant linear association, Figure 3 shows relationship curves between hemispheric CBF values and age, as determined with distance-weighted least-squares smoothing method, because of crucial age dependence changes in normal healthy children as reported using positron emission tomography (PET) method [16] or perfusion CT [17].

Sedated patients had slightly higher median SPO_2 values than un-sedated children: 99% (95-100%) vs. 95% (90-100%); p<.001.

Table 1 Demographic and clinical data of 42 children with sickle cell anemia classified as having low risk of stroke by transcranial Doppler ultrasonography criteria (mean blood flow velocity <170 cm/s) who underwent magnetic resonance continuous arterial spin labeling imaging examinations.

Variable	All children	Female	Male	Difference p value
	N=42	N=24	N=18	0.355§
Age (years)	8.1±3.3	8.2±3.7	8.0±2.9	0.890†
Hemoglobin (g/dL)	8.3±1.1	8.4±0.8	8.2±1.4	0.515†
Hematocrit (%)	24.5±3.5	24.5±2.9	23.5±4.3	0.381†
Heart rate (1/min)	85 (58;153)	88 (68;153)	84 (58;98)	0.022*
Systolic blood pressure (mm Hg)	104±11	102±10	105±12	0.494†
Diastolic blood pressure (mm Hg)	51±10	50±10	52±11	0.509†
Mean arterial pressure (mm Hg)	69±9	68±9	70±10	0.448†
SPO_2 (%)	98 (90;100)	97 (90;100)	98 (93;100)	0.304*

Data are: mean ± standard deviation or median (minimum and maximum in parentheses).
SPO_2 - Capillary blood oxygen saturation (pulse oximetry).
Statistics: § Pearson $\updownarrow^2$, † *t*-test with unequal variances, * Mann-Whitney *U* test.

Table 2 Mean values and limits of Gaussian tolerance interval of cerebral blood flow (CBF) obtained with continuous spin arterial labeling MR imaging in 42 children with sickle cell anemia, classified as having low risk of stroke by transcranial Doppler ultrasonography criteria (mean blood flow velocity in main cerebral arteries <170 cm/s).

CBF	Whole brain	Right hemisphere	Left hemisphere	Difference (p value)
mean ± SD	83±19	82±20	84±19	0.119
Limits of tolerance interval	40 - 126	36 - 127	41 - 127	0.119

Data are: ml/100g/min; statistics: paired 2-sided *t*-test

Discussion

Our study provides for the first time tolerance reference intervals for CASL MR perfusion values for total brain as well as for each hemisphere. The intervals were calculated on the basis of data obtained from a carefully selected homogenous cohort of children with sickle cell anemia, who were classified as children with a low risk of stroke. Therefore, the reference intervals would be useful to identify children with a greater risk of stroke than those from our cohort. However, this hypothesis needs to be verified in a separate study, likely one similar in design to the STOP study. Specifically, reference intervals of CASL MR perfusion provide thresholds that can be considered useful to estimate the risk of clinical and subclinical stroke if confirmed by a prospective study. As anatomical MRI and MRA studies are being performed in most university medical centers as part of a screening program of children with SCA, adding an MR perfusion study would provide unique new possibilities in the assessment of stroke risk.

Despite of the use of a homogenous cohort of children with SCA, our reference intervals cover a rather wide spectrum of perfusion values. CBF and systemic circulation in SCA must be adapted to the abnormal rheologic behavior of sickle cells, but they are also under the influence of many other biological and technical factors such as viscosity. Blood viscosity is a function of the number of red blood cells (RBC), their deformability and the makeup of plasma proteins. In SCA, blood viscosity is dominated by the polymerization of hemoglobin S and the presence of dense sickle cells. At a hematocrit of 25%, the viscosity is only slightly lower than that of normal blood (45%) [18]. Upon deoxygenation below 85%, the viscosity rises sharply, because of the polymerization of deoxy-HbS [18]. Reduced viscosity in SCA partially protects the microcirculatory flow, which as indicated in the Hagen-Poiseuille equation, is directly proportional to pressure and inversely proportional to viscosity. A 50% increase in blood viscosity increases total peripheral resistance by 75% and reduces flow unless the ABP rises to compensate [19]. Hematocrit is, therefore, along

with ABP and HR, an important factor that can affect CBF. Any viscosity increase is most likely counterbalanced by vasodilatation to ensure oxygen delivery. According to the vascular network model [20], faster blood flow through the cerebral microvasculature lowers oxygen extraction and increases venous hemoglobin oxygen saturation. Higher CBF with relatively lower concentration of deoxy-HbS in capillaries is probably protective, as the viscosity of blood carrying RBCs containing deoxy-HbS is tenfold higher than with oxyhemoglobin [19]. When CBF decreases and velocity in capillaries drops, the oxygen extraction can increase from 35%-45% to more than 90% [21], with a resulting increase in deoxy-HbS and a subsequent increase in HbS polymerization. "Stickier" blood then travels to the end of capillaries and the venous system. Despite a dramatic blood pressure increase, the viscosity may rise to levels that cause blood flow to be essentially stationary.

Even a minor stenosis of a large artery can pose a major challenge for the already compromised CBF. The perfusion pressure and velocity drop downstream to stenosis, which probably enhances oxygen extraction at the tissue level and locally increases concentration of deoxy-HbS causing an increase in blood viscosity. Therefore, in our cohort it was important to exclude children with even minor intracranial narrowings.

We demonstrated that absolute CBF was higher in our cohort than in reported healthy children [12], supporting the hypothesis of relative hyperemia in children with SCA as a result of chronic anemia. These findings are consistent with previously published studies of CBF in children with SCA with the use of CASL MRI as well as other imaging techniques such as Xenon-enhanced CT (Xe-CT) or PET [6,11,21-25].

In the present study, CASL MR perfusion imaging was employed to assess CBF at the tissue level. CASL MR utilizes endogenous spin-labeled arterial blood protons, as opposed to injected contrast (gadolinium), to quantify CBF. Only a few studies [6,11,12,24,25] have demonstrated potential benefits of CASL MR in the evaluation of CBF in children with SCA. As with every technique, CASL MRI has inherent limitations. A potential error in CBF quantification is related to employing perfusion models with physiologic parameters derived from adults [12].

In the single compartment model, assuming that all of the labeled blood stays in the vasculature, perfusion errors arise mainly from the choice of two parameters: the T1 of blood

(T1a) and the blood brain partition coefficient of water. Blood T1 in children is expected to be longer than the adult value because the blood water content is higher than in adults [26]. As a result, adopting adult blood T1 for perfusion quantification in children may lead to overestimation of CBF. Conversely, previous data suggest that the blood brain partition coefficient of water is greater in children (1.1 mL/g in neonates) [26] than in adults (0.9 mL/g), which would cause underestimation of child CBF by using the adult parameters. Because the effects of T1 and T1a tend to be counterbalanced by each other, the adult perfusion model provides a reasonable approximation of child CBF quantification, and yields CBF measures that are comparable to values obtained using radioactive methods [27]. Based on simulation, the overall error is approximately 5% across the entire age span (0-18 years). Given the sparse literature and large variability of these parameters in pediatric age groups, CBF quantification based on adult perfusion models seems to be a reasonable solution. Nevertheless, optimizing the specific perfusion model for pediatric populations bears considerable importance and significance in clinical diagnosis because these parameters may vary with the pathologic state. Recent literature also suggests that the two compartment perfusion model, which takes into account the limited water exchange (permeability) between capillary and brain tissue, may provide a more accurate perfusion estimation compared with the single compartment model [28]. The two compartment perfusion model involves more parameters that may vary with age, such as the permeability surface (PS) product and the T2/T2* of blood and brain tissue. Several other limitations of the CASL MR method have been reviewed by Peterson et al. [29].

Average side-to-side differences in hemodynamic parameters in adults were reported to be negligible; thus, substantial inter-hemispheric asymmetry is commonly interpreted as a sign of arterial narrowing [30-34]. The statistical average group difference cannot be applied to an individual, in whom the exact configuration of the circle of Willis [35], including the presence, caliber, and course of each artery [36,37], and the degree of inter-hemispheric anatomic [38-40], physiologic [41-43], and functional differences are *a priori* unknown [6,32,36,44]. Large variability in side-to-side perfusion values and less than perfect correlation coefficients for hemispheres that are "seeing" the same circulating oxygen content and Hgb indicate that there is not such

a tight agreement between sides in blood flow redistributions in response to a chronic oxygen deficit [22,23,44,45].

In our cohort we did not find age dependency of CBF as reported in healthy children [16,17]. The slope of age dependency however, was flatter in children with SCA (Figure 2). Such dissociation between CBF and age in children with SCA can be explained by the effect of hyperdynamic circulation associated with lower Hct and Hgb [23,46,47]. We also did not find a significant relationship between CBF and hematologic parameters. The effect is most likely related to small variability of hematologic parameters in our cohort of relatively homogenous "healthy" children in steady state.

As in healthy children, sex differences in CBF were not observed in our group [48,49]. Two other reports, however, did show these differences [50,51], which were explained by sex differences in cerebrovascular resistance and vascular reactivity. In children with SCA, altered resistance and reactivity may counterbalance sex differences in CBF [52-54].

Broad reference tolerance intervals can be related to the sample size in our study, which is relatively small compared with studied groups of healthy children. The National Committee for Clinical Laboratory Standards recommends that the sample size should consist of at least 120 values [55,56]. The Committee recognizes, however, that in a special category of individuals, 39 observations is the required minimum to compute a 95% reference interval at 2.5% and 97.5% of the points of the distribution.

Conclusions

This study provides reference tolerance limits of CBF values as measured using CASL MR perfusion imaging for the whole brain and for each hemisphere in children with SCA. The limits can be helpful in the identification of children at higher risk of brain ischemia.

Acknowledgement

References

1 Platt O, Brambilla D, Rosse W, et al. Mortality in sickle cell disease. Life expectancy and risk factors for early death. N Engl J Med. 1994; 330: 1639-1644.
2 Powars DR, Chan LS, Hiti A, et al. Outcome of sickle cell anemia: a 4-decade observational study of 1056 patients. Medicine (Baltimore). 2005; 84: 363-376.
3 Pegelow C, Macklin E, Moser F, et al. Longitudinal changes in brain magnetic resonance imaging findings in children with sickle cell disease. Blood. 2002; 99: 3014-3018.
4 Miller S, Macklin E, Pegelow C, et al. Silent infarction as a risk factor for overt stroke in children with sickle cell anemia: a report from the Cooperative Study of Sickle Cell Disease. J Pediatr. 2001; 139: 385-390.
5 Serjeant GR. Sickle-cell disease. Lancet. 1997; 350: 725-730.
6 van den Tweel XW, Nederveen AJ, Majoie CB, et al. Cerebral blood flow measurement in children with sickle cell disease using continuous arterial spin labeling at 3.0-Tesla MRI. Stroke. 2009; 40: 795-800.
7 Buchanan ID, James-Herry A, Osunkwo I. The Other Side of Abnormal: A Case Series of Low Transcranial Doppler Velocities Associated With Stroke in Children With Sickle Cell Disease. J Pediatr Hematol Oncol. 2012.
8 Alsop DC, Detre JA. Reduced transit-time sensitivity in noninvasive magnetic resonance imaging of human cerebral blood flow. J Cereb Blood Flow Metab. 1996; 16: 1236-1249.
9 Alsop DC, Detre JA. Multisection cerebral blood flow MR imaging with continuous arterial spin labeling. Radiology. 1998; 208: 410-416.
10 Gevers S, Nederveen AJ, Fijnvandraat K, et al. Arterial spin labeling measurement of cerebral perfusion in children with sickle cell disease. J Magn Reson Imaging. 2012; 35: 779-787.
11 Strouse JJ, Cox CS, Melhem ER, et al. Inverse correlation between cerebral blood flow measured by continuous arterial spin-labeling (CASL) MRI and neurocognitive function in children with sickle cell anemia (SCA). Blood. 2006; 108: 379-381.
12 Wang J, Licht DJ. Pediatric perfusion MR imaging using arterial spin labeling. Neuroimaging Clin N Am. 2006; 16: 149-167, ix.
13 Aaslid R, Markwalder TM, Nornes H. Noninvasive transcranial Doppler ultrasound recording of flow velocity in basal cerebral arteries. J Neurosurg. 1982; 57: 769-774.
14 Lumsden JH, Mullen K. On establishing reference values. Can J Comp Med. 1978; 42: 293-301.
15 Weissberg AB, Beatty GH. Tables of tolerance limit factors for the normal distribution. Technometrics. 1960; 2 (4): 483-500.
16 Takahashi T, Shirane R, Sato S, et al. Developmental changes of cerebral blood flow and oxygen metabolism in children. Am J Neuroradiol. 1999; 20: 917-922.
17 Wintermark M, Lepori D, Cotting J, et al. Brain perfusion in children: evolution with age assessed by quantitative perfusion computed tomography. Pediatrics. 2004; 113: 1642-1652.
18 Chien S. Rheology of sickle cells and the microcirculation. N Engl J Med. 1984; 311: 1567-1569.
19 Johnson CS. Arterial blood pressure and hyperviscosity in sickle cell disease. Hematol Oncol Clin North Am. 2005; 19: 827-837, vi.
20 Boas DA, Jones SR, Devor A, et al. A vascular anatomical network model of the spatio-temporal response to brain activation. Neuroimage. 2008; 40: 1116-1129.

21 Herold S, Brozovic M, Gibbs J, et al. Measurement of regional cerebral blood flow, blood volume and oxygen metabolism in patients with sickle cell disease using positron emission tomography. Stroke. 1986; 17: 692-698.

22 Prohovnik I, Hurlet-Jensen A, Adams R, et al. Hemodynamic etiology of elevated flow velocity and stroke in sickle-cell disease. J Cereb Blood Flow Metab. 2009; 29: 803-810.

23 Prohovnik I, Pavlakis SG, Piomelli S, et al. Cerebral hyperemia, stroke, and transfusion in sickle cell disease. Neurology. 1989; 39: 344-348.

24 Oguz KK, Golay X, Pizzini FB, et al. Sickle cell disease: continuous arterial spin-labeling perfusion MR imaging in children. Radiology. 2003; 227: 567-574.

25 Helton KJ, Paydar A, Glass J, et al. Arterial spin-labeled perfusion combined with segmentation techniques to evaluate cerebral blood flow in white and gray matter of children with sickle cell anemia. Pediatr Blood Cancer. 2009; 52: 85-91.

26 Herscovitch P, Raichle ME. What is the correct value for the brain--blood partition coefficient for water? J Cereb Blood Flow Metab. 1985; 5: 65-69.

27 Chiron C, Raynaud C, Mazière B, et al. Changes in regional cerebral blood flow during brain maturation in children and adolescents. J Nucl Med. 1992; 33: 696-703.

28 St Lawrence KS, Wang J. Effects of the apparent transverse relaxation time on cerebral blood flow measurements obtained by arterial spin labeling. Magn Reson Med. 2005; 53: 425-433.

29 Petersen ET, Zimine I, Ho YC, et al. Non-invasive measurement of perfusion: a critical review of arterial spin labelling techniques. Br J Radiol. 2006; 79: 688-701.

30 Adams R, McKie V, Hsu L, et al. Prevention of a first stroke by transfusions in children with sickle cell anemia and abnormal results on transcranial Doppler ultrasonography. N Engl J Med. 1998; 339: 5-11.

31 Adams R, Nichols F, Figueroa R, et al. Transcranial Doppler correlation with cerebral angiography in sickle cell disease. Stroke. 1992; 23: 1073-1077.

32 Brint SU, Al-Khalidi HR, Vatel B, et al. MCA flow asymmetry is a marker for cerebrovascular disease. Neurol Res. 1996; 18: 163-167.

33 Grolimund P, Seiler RW, Aaslid R, et al. Evaluation of cerebrovascular disease by combined extracranial and transcranial Doppler sonography. Experience in 1,039 patients. Stroke. 1987; 18: 1018-1024.

34 Sorteberg W, Langmoen IA, Lindegaard KF, et al. Side-to-side differences and day-to-day variations of transcranial Doppler parameters in normal subjects. J Ultrasound Med. 1990; 9: 403-409.

35 Riggs HE, Rupp C. Variation in form of circle of Willis. The relation of the variations to collateral circulation: anatomic analysis. Arch Neurol. 1963; 8: 8-14.

36 Krejza J, Mariak Z, Babikian V. Importance of angle correction in the measurement of blood flow velocity with transcranial Doppler sonography. Am J Neuroradiol. 2001; 22: 1743-1747.

37 Zurada A, St Gielecki J, Tubbs RS, et al. Three-dimensional morphometry of the A1 segment of the anterior cerebral artery with neurosurgical relevance. Neurosurgery. 2010; 67: 1768-1782; discussion 1782.

38 Chen R, Pawlak MA, Flynn TB, et al. Brain morphometry and intelligence quotient measurements in children with sickle cell disease. J Dev Behav Pediatr. 2009; 30: 509-517.

39 Thoma RJ, Yeo RA, Gangestad SW, et al. Fluctuating asymmetry and the human brain. Laterality. 2002; 7: 45-58.

40 Watkins KE, Paus T, Lerch JP, et al. Structural asymmetries in the human brain: a voxel-based statistical analysis of 142 MRI scans. Cereb Cortex. 2001; 11: 868-877.

41 Hendrikse J, van Raamt A, van der Graaf Y, et al. Distribution of cerebral blood flow in the circle of Willis. Radiology. 2005; 235: 184-189.

42 Vallortigara G. The evolutionary psychology of left and right: costs and benefits of lateralization. Dev Psychobiol. 2006; 48: 418-427.

43 Schaafsma SM, Riedstra BJ, Pfannkuche KA, et al. Epigenesis of behavioural lateralization in humans and other animals. Philos Trans R Soc Lond B Biol Sci. 2009; 364: 915-927.

44 Sette G, Baron JC, Mazoyer B, et al. Local brain haemodynamics and oxygen metabolism in cerebrovascular disease. Positron emission tomography. Brain. 1989; 112 (Pt 4): 931-951.

45 Ausavarungnirun P, Sabio H, Kim J, et al. Dynamic vascular analysis shows a hyperemic flow pattern in sickle cell disease. J Neuroimaging. 2006; 16: 311-317.

46 Lee M, Piomelli S, Granger S, et al. Stroke Prevention Trial in Sickle Cell Anemia (STOP): extended follow-up and final results. Blood. 2006; 108: 847-852.

47 Hayashi K, Handa H, Nagasawa S, et al. Stiffness and elastic behavior of human intracranial and extracranial arteries. J Biomech. 1980; 13: 175-184.

48 Schoning M, Staab M, Walter J, et al. Transcranial color duplex sonography in childhood and adolescence. Age dependence of flow velocities and waveform parameters. Stroke. 1993; 24: 1305-1309.

49 Schoning M, Hartig B. The development of hemodynamics in the extracranial carotid and vertebral arteries. Ultrasound Med Biol. 1998; 24: 655-662.

50 Vavilala MS, Kincaid MS, Muangman SL, et al. Gender differences in cerebral blood flow velocity and autoregulation between the anterior and posterior circulations in healthy children. Pediatr Res. 2005; 58: 574-578.

51 Tontisirin N, Muangman S, Suz P, et al. Early childhood gender differences in anterior and posterior cerebral blood flow velocity and autoregulation. Pediatrics. 2007; 119: E610-E615.

52 Brown MM, Wade JP, Marshall J. Fundamental importance of arterial oxygen content in the regulation of cerebral blood flow in man. Brain. 1985; 108 (Pt 1): 81-93.

53 Reiter CD, Wang X, Tanus-Santos JE, et al. Cell-free hemoglobin limits nitric oxide bioavailability in sickle-cell disease. Nat Med. 2002; 8: 1383-1389.

54 Van Mil AH, Spilt A, Van Buchem MA, et al. Nitric oxide mediates hypoxia-induced cerebral vasodilation in humans. J Appl Physiol. 2002; 92: 962-966.

55 Horn PS, Pesce AJ. Reference intervals: an update. Clin Chim Acta. 2003; 334: 5-23.

56 National Committee for Clinical Laboratory Standards. How to define and determine reference intervals in the clinical laboratory: approved guideline. NCCLS document C28-A and C28-A2. Villanova, PA: National Committee for Clinical and Laboratory Standards (NCCLS); 1995, 2001.

Michal Arkuszewski, MD, PhD
Department of Neurology
Medical University of Silesia
Central University Hospital
Medykow 14
40-752 Katowice, Poland
Tel.: +48 32 789 46 01
Fax: +48 32 789 45 55
E-mail: michal.arkuszewski@gmail.com